Conversion of a Cosubstrate to an Inhibitor: Phosphorylation Mutants of Nicotinic Acid Phosphoribosyltransferase†

Mathumathi Rajavel,‡,§ Dominique Lalo,||,⊥ Jeffrey W. Gross,‡ and Charles Grubmeyer*,‡

Fels Research Institute and Department of Biochemistry, Temple University School of Medicine, 3307 North Broad Street, Philadelphia, Pennsylvania 19140, and Service de Biochemie Genetique Moleculaire, CEA Saclay, F91191, France

Received August 13, 1997

ABSTRACT: Nicotinic acid phosphoribosyltransferase (NAPRTase; EC 2.4.2.11) forms nicotinic acid mononucleotide (NAMN) and PP_i from 5-phosphoribosyl 1-pyrophosphate (PRPP) and nicotinic acid (NA). The V_{max} NAMN synthesis activity of the *Salmonella typhimurium* enzyme is stimulated about 10-fold by ATP, which, when present, is hydrolyzed to ADP and P_i in 1:1 stoichiometry with NAMN formed. The overall NAPRTase reaction involves phosphorylation of a low-affinity form of the enzyme by ATP, followed by generation of a high-affinity form of the enzyme, which then binds substrates and produces NAMN. Hydrolysis of E−P then regenerates the low-affinity form of the enzyme with subsequent release of products. Our earlier studies [Gross, J., Rajavel, M., Segura, E., and Grubmeyer, C. (1996) *Biochemistry 35*, 3917−3924] have shown that His-219 becomes phosphorylated in the N1 (π) position by ATP. Here, we have mutated His-219 to glutamate and asparagine and determined the properties of the purified mutant enzymes. The mutant NAPRTases fail to carry out ATPase, autophosphorylation, or ADP/ATP exchanges seen with wild-type (WT) enzyme. The mutants do catalyze the slow formation of NAMN in the absence of ATP with rates and K_M values similar to those of WT. In striking contrast to WT, NAMN formation by the mutant enzymes is competitively inhibited by ATP. Thus, the NAMN synthesis reaction may occur at a site overlapping that for ATP. Previous studies suggest that the yeast NAPRTase does not catalyze NAMN synthesis in the absence of ATP. We have cloned, overexpressed, and purified the yeast enzyme and report its kinetic properties, which are similar to those of the bacterial enzyme.

Salvage pathways for NAD formation (*1*, *2*) utilize the enzyme NAPRTase,[1] whose interaction with ATP is bioenergetically intriguing. NAPRTase (EC 2.4.2.11) catalyzes the formation of the nucleosidic bond between ribose 5-phosphate of PRPP and nicotinic acid to form PP_i and the penultimate NAD precursor NAMN. Like the other nine PRTases that act to form the purine, pyrimidine, and pyridine nucleotides, as well as the nucleotidelike intermediates of histidine and tryptophan biosynthesis (*3*), NAPRTase utilizes PRPP and shows a high degree of base specificity.

Little is known about NAPRTase structure. A previously identified 14-residue sequence motif (*4, 5*), found in PRPP synthase as well as several of the PRTases, suggested a common evolutionary origin for these enzymes. Recent crystallographic studies by our collaborators (*6, 7*) and other groups (*8*) have shown that three of the PRTases follow a Rossman-like five-stranded α/β fold, now designated the type 1 PRTase fold, with the conserved sequence motif at its center, where it interacts with the ribose hydroxyls and 5-phosphate of PRPP, confirming its previously assigned function in PRPP binding. However, the sequences of the *Escherichia coli* and *Salmonella typhimurium* forms of NAPRTase (*9, 10*) and of *S. typhimurium* quinolinate PRTase (*11*) failed to reveal similarity to the PRPP binding motif. The sequence information suggests an evolutionary origin (or origins) for the pyridine PRTases that may be distinct from those PRTases that contain the nucleotide fold. In accord with this view, the recent crystal structure of QAPRTase (*12*) has revealed a fundamentally different α/β barrel architecture, designated the type 2 PRTase fold.

A second difference between NAPRTase and the other PRTases lies in its use of ATP. It is known that ATP stimulates NAMN formation by NAPRTase from several sources (*13*−*19*), and that stimulation is accompanied by hydrolysis of ATP stoichiometric to NAMN formed (*15*, *17*−*19*). Although some of the other PRTases show allosteric stimulation by effector molecules (*3*), including GTP (*20*, *21*), NAPRTase is the only PRTase known to cleave the stimulator during the reaction cycle. The facultative hydrolysis of ATP raises important questions about NAPRTase

† This research was supported by a grant from the National Science Foundation (DMB91-03029) to C.G. J.G. is a recipient of federal work study funds.

* To whom correspondence should be addressed: Phone 215-707-4495; FAX 215-707-7536; email ctg@ariel.fels.temple.edu.

‡ Temple University School of Medicine.

§ Present address: Department of Biochemistry, Johns Hopkins University, 615 N. Wolfe St., Baltimore MD 21205.

|| CEA Saclay.

⊥ Present address: Department of Biological Chemistry, University of California, Irvine, CA 92717.

[1] Abbreviations: WT, wild-type enzyme; NA, nicotinic acid; NAMN, nicotinic acid mononucleotide; PRTase, phosphoribosyltransferase; NAPRTase, nicotinic acid phosphoribosyltransferase; PRPP, α-D-5-phosphoribosyl 1-pyrophosphate; PP_i, pyrophosphate; QAPRTase, quinolinic acid phosphoribosyltransferase.

S0006-2960(97)02013-8 CCC: $15.00
Published on Web 02/28/1998

energetics. We have shown that a "steady-state" energy coupling between ATP hydrolysis and NAMN formation exists in the *S. typhimurium* enzyme, in which ATP hydrolysis serves to drive NAMN formation far toward products (*19*). However, in contrast to the behavior of equilibrium coupled systems, complete hydrolysis of the ATP is followed by rapid net pyrophosphorolysis of NAMN, without resynthesis of ATP.

How does ATP hydrolysis drive NAMN formation in NAPRTase? It is not likely that the coupling involves a reaction intermediate formed by the phosphorylation of either substrate. Such chemical coupling (*22*) is easily understood and is found in a variety of enzymes, including glutamine synthetase (*23*). The alternative mechanisms do not employ substrate-linked phosphorylation (*22, 24, 25*) but instead use the steps of ATP hydrolysis to drive enzyme-linked differential molecular discrimination. The enzyme allows favorable binding or catalytic properties at discrete reaction steps and disallows them at others. This coupling strategy was originally proposed to explain the operation of ATP-driven ion pumps, but recent work has uncovered a panoply of additional ATPases that use molecular discrimination, including many involved in macromolecular recognition and processing (*26, 27*). The questions concerning energetic coupling through molecular discrimination are thus of considerable importance, and NAPRTase constitutes an ideal model system for their study.

Kinetic studies and ADP/ATP exchanges led us to propose that NAPRTase becomes covalently phosphorylated by ATP. Recently, we have found that enzyme phosphorylation occurs at His-219, forming the labile 1-phosphohistidine form of that residue (*28*). Phosphorylation at His-219 was chemically and kinetically competent to participate in the steady-state reaction. Concomitant with ATP binding and enzyme phosphorylation, the enzyme attains a state with high affinity for PRPP and NA substrates. NAMN formation and hydrolysis of E−P then occur, resulting in the relaxation to the low-affinity state, and release of products. The alternation of apoenzyme and phosphoenzyme states thus allows NAPRTase to bind its substrates selectively from low concentration and release products against a high concentration. In support of the proposed ATP-induced conformational change, we have shown that, in the presence of ATP, a 25-residue trypsin-sensitive segment of the carboxyl terminal becomes protected from proteolysis (*27*). The trypsin-cleaved enzyme is inactive for ATP-linked functions and loses NAMN synthesis activity as well. However, the relationship between the ATPase and NAMN synthesis active sites has not yet been delineated. It could be that they occupy separate contiguous parts of the sequence and are largely structurally independent (a domain relationship) or it could be that the functions overlap in sequence and/or in the folded protein.

The relationship between the NAMN and ATP sites can be explored through the alternative reactions catalyzed by the *S. typhimurium* enzyme. The bacterial enzyme catalyzes a slow NAMN synthesis in the absence of ATP and a rapid ATPase in the presence of PP_i. Although the mammalian enzyme also shows NAMN synthesis in the absence of ATP (*18*), it has been reported that the yeast enzyme does not catalyze this reaction (*29*). Additionally, NAMN, as well as PP_i, was reported to trigger ATP hydrolysis by the yeast enzyme; this NAMN-stimulated activity was not identified in studies of the bacterial enzyme (*19*). The differences between the yeast and *S. typhimurium* enzymes suggested that the alternative reactions might not reflect intrinsic properties of the system but arise as artifacts of enzyme preparation.

In the current work we have undertaken mutagenesis experiments at His-219, both to confirm its role in phosphorylation and to investigate the relationship between ATPase and NAMN synthesis. As predicted, the ATP-linked functions of the enzyme were inactivated by mutation of His-219 to glutamate or asparagine. However, the NAMN synthesis activity of the enzyme in the absence of ATP was largely unaffected and retained similar K_M values. Surprisingly, in these mutant enzymes, ATP became an inhibitor of the NAMN synthesis activity. We have also overproduced and purified the yeast enzyme, and report that the alternative reactions are similar to those of the *Salmonella* enzyme.

EXPERIMENTAL PROCEDURES

Materials. Bacterial growth media were from Difco. Restriction enzymes and T4 DNA ligase were obtained from New England Biolabs. Taq DNA polymerase and dNTPs were purchased from Perkin-Elmer. Sequenase was from USB. Lactate dehydrogenase and pyruvate kinase were from Boehringer Mannheim. P^1,P^5-Di(adenosine-5′-) pentaphosphate, [^{14}C]nicotinic acid, [^{14}C]ADP, and other biochemicals were obtained from Sigma. [γ-^{32}P]ATP was purchased from Amersham, and [^{32}P]PP_i and [α-^{35}S]ATP were from DuPont−NEN. Inorganic chemicals and chromatography solvents were purchased from Fisher. Customized primers were synthesized at the DNA synthesis facility of Temple University School of Medicine and Ransom Hill Bioscience Inc. T7 primers used for *pncB* sequencing were obtained from Novagen. Preparation of [β-^{32}P]PRPP for binding studies followed procedures of Xu et al. (*30*).

Bacterial Strains, Plasmids, and Culture Conditions. All strains were grown at 37 °C with the exceptions of RMS100 (JF1024/pGP1-2), RMS01, RM219E, and RM219N, which were grown at 30 °C, and RMS12, at 25 °C. *S. typhimurium* RM926 [*hsdLT*(r^- m^+) *hsdSA*(r^- m^+) *metE551 trpD2 leu val rpsL120 galE*] was donated by Russell Maurer, Case Western Reserve University, and *S. typhimurium* JF1024 (Δ*nadA141 gal*$^-$ Δ*pncB3 metP70 recA1* Δ*srl*) was obtained from John Foster, University of South Alabama. DH5α F^- [ϕ80d*lac*Δ(*lacZ*)M15) Δ(*lacZYA*−*argF*)U169 *deoR endA1 hsdR17*(r_k^- m_k^+) *phoA supE44* λ^- *thi-1 recA1 gyrA relA1*] was used as the initial host for cloning the yeast NAPRTase gene, *npt1*. BL21(DE3) [F^- *ompT hsdS*$_B$(r_B^- m_B^-); an *E. coli* B strain] with a λ prophage carrying the T7 RNA polymerase gene was used for overproducing yeast *npt1*. Yeast *npt1* contained in plasmid pFL44-RPB10f was constructed as described (*31*). pRM1-1, pRM1-2, pRM219E, and pRM219N constructed in this study are described below. Plasmid pRSETC was from Invitrogen and plasmid pGP1-2 (*32*) was a gift from Stanley Tabor, Harvard Medical School. Plasmid pRM17.1 was desribed by Rajavel et al. (*27*).

Conventional recombinant DNA techniques were performed as described in Sambrook et al. (*33*). DNA purification was carried out with Qiagen plasmid purification kits. Dideoxy DNA sequencing with Sequenase and PCR reac-

tions with Taq polymerase were carried out as described by the manufacturers in a Coy thermal cycler.

Construction of npt1 Overexpression Plasmid. A 1.4 kb *Bam*HI/*Pvu*II fragment from pFL44-RPB10f encoding *npt1* was ligated to similarly digested pRSETC vector. *E. coli* DH5α was transformed with the ligated mixture and the positive clone (pRM1-1) carrying the insert was identified by restriction digestion. The *npt1* coding sequence was PCR-amplified from pRM1-1 using DNA oligomers (clockwise primer 5′ GCAAGATAACATATGTCAGAACC 3′ and counterclockwise T7 termination primer 5′ GCTAGTTATTGCTCAGCGG 3′). The clockwise primer contained a restriction site (underlined) for *Nde*I. The amplified fragment was digested with *Nde*I/*Mun*I and the 120 bp fragment was ligated to similarly digested pRM1-1. *E. coli* DH5α was transformed with the ligated mixture and the resultant construct, designated pRM1-2, was sequenced at the 5′ end of the gene across the *Mun*I restriction site (120 bp) to ensure that no undesired mutations had occurred during PCR amplification. *E. coli* BL21(DE3) was transformed with pRM1-2 and the resultant strain (RMS12) gave high level expression of *npt1*.

Construction and Purification of pncB Mutants. Mutations were made using overlap PCR (*34*). The mutagenic primers (the underlined bases encode the desired amino acid) were as follows: H219E clockwise, 5′ GGCACTCAGGCGGAAGAATGGTTC 3′; H219E counterclockwise, 5′ GGAACCATTCTTCCGCCTGAGTGCC 3′; H219N clockwise, 5′ GGCACTCAGGCGAACGAATGGTTCC 3′; H219N counterclockwise, 5′ GGAACCATTCGTTCGCCTGAGTGCC 3′. The end primers (*27*) contained restriction sites for *Nde*I and *Nco*I. Amplification of the mutagenic DNA fragments from the wild-type plasmid template (pRM17.1) was achieved by adding 50 ng of template DNA and 100 pmol each of the desired mutagenic primers and end primers in a typical PCR reaction. The samples were subjected to 35 cycles of denaturation (1 min, 92 °C), annealing (5 min, 55 °C), and extension (2 min, 72 °C). The product of each PCR reaction was purified with agarose gel electrophoresis followed by Geneclean (Bio101). The DNA fragments carrying the overlapping sequence of the desired mutation were then amplified under similar conditions using only the end primers. The entire coding sequence carrying the desired mutation was then excised with *Nde*I and *Nco*I and ligated with similarly digested pRM17.1, thus replacing the wild-type fragment with the mutant fragment. An initial transformation was carried out in *S. typhimurium* RM926. The mutant plasmids (designated pRM219E and pRM219N) were sequenced across the entire coding region to ensure that no undesired mutations had occurred during PCR amplification. *S. typhimurium* RMS100 was transformed with pRM219E and pRM219N and the resultant strains, RMS219E and RMS219N, gave high-level expression of mutant *pncB*.

Purification of Yeast and Mutant NAPRTase. The purification of yeast NAPRTase followed the method described earlier for the *S. typhimurium* enzyme (*27*). The yeast protein eluted at approximately 0.4 M NaCl on the Q-Sepharose column and at 22% $(NH_4)_2SO_4$ saturation on the phenyl-Sepharose column. The active fractions showed negligible ATPase activity in the absence of NA. The purification of mutant NAPRTases was followed by SDS−PAGE. The purified enzymes were stored at 4 °C as 70% saturated ammonium sulfate suspensions in 200 mM NaP_i buffer, pH 8.0, containing 10% glycerol and 5 mM DTT. Analysis on SDS−10% PAGE showed a high degree of homogeneity.

Assay of Enzymatic Activity. Coupled spectrophotometric ATPase assays were performed as described by Vinitsky and Grubmeyer (*19*). The PP_i- and NAMN-stimulated ATPase assays were conducted as for coupled ATPase, except PRPP was omitted and either 1 mM PP_i or 1 mM NAMN was added. In the NAMN-stimulated ATPase assays, yeast inorganic pyrophosphatase was added to verify that the ATPase activity was not caused by PP_i contamination of the NAMN. The [^{14}C]NA label transfer procedure of Preiss and Handler (*35*) was performed in a 0.1 mL total volume at 30 °C and quantified by phosphoimaging as described by Rajavel et al. (*27*). Protein measurements were done spectrophotometrically using $E^{0.1\%}_{280nm} = 1.65$ for the *S. typhimurium* enzyme (*36*) and 1.27 for the yeast enzyme. A unit of activity is defined as that amount of enzyme catalyzing the conversion of 1 μmol of NA or ATP/min under the conditions given.

Enzyme Phosphorylation. Yeast and *S. typhimurium* NAPRTase were phosphorylated with [γ-^{32}P]ATP as described by Gross et al. (*28*) except that covalently bound ^{32}P was separated from unreacted [γ-^{32}P]ATP by passage through a G-50 centrifuge column (*37*) preequilibrated in 200 mM potassium glutamate, 20 mM Tris base, and 1 mM NaP_i, pH 8.3, containing 6 M urea.

Physical Properties. Enzyme samples (50 μL) at 10 mg/mL in 200 mM NaP_i, pH 8.0, 5% glycerol, 1 mM EDTA, and 2 mM DTT were chromatographed on Superdex-75 (1 × 30 cm) preequilibrated in the same buffer and eluted at 0.5 mL/min. Electrospray mass spectrometry was carried out by Dr. William Moore at the University of Pennsylvania, on samples prepared by HPLC as described by Rajavel et al. (*27*). Amino-terminal protein sequencing of the yeast enzyme was performed as described by Rajavel et al. (*27*).

Kinetic Parameters of Mutant NAPRTases. Assays of enzymatic activity were performed as described by Rajavel et al. (*27*). Kinetic constants for uncoupled NAMN synthesis were determined from steady-state initial rate measurements with NA and PRPP as substrates. For K_M determinations with PRPP, and in assays where ATP inhibition was monitored, the amount of $MgSO_4$ was adjusted to keep a constant 3 mM excess Mg^{2+} over the substrates ATP and PRPP. All measurements were carried out at 30 °C and chromatograms were analyzed using phosphorimaging (*27*). The kinetic data were fit to the hyperbolic form of the Michaelis−Menten equation using the programs developed by Cleland (*38*). ADP/ATP exchange reactions were carried out as described (*19*) using [^{14}C]ADP.

Equilibrium Gel Filtration. The approach of Hummel and Dreyer (*39*), as modified (*30*), was used to quantitate ligand binding. NAPRTase (100−380 μM) binding to either [β-^{32}P]-PRPP (100 μM) or [^{32}P]PP_i (25 μM−1.5 mM) was assayed in 200 mM potassium glutamate, 20 mM Tris, pH 8.3, 3 mM $MgCl_2$, 5 mM DTT, and [^{3}H]glucose. Where indicated, the reactions were supplemented with 5 mM MgATP. The binding of ligand to NAPRTase was plotted as described by Scatchard (*40*). The *S. typhimurium* enzyme is monomeric (*41*) with M_r = 45 529, and all molarities refer to the monomeric molecule.

Partial Proteolysis of NAPRTase. NAPRTases were subjected to trypsin as described in Rajavel et al. (*27*).

RESULTS

Mutagenesis and Purification of Mutant NAPRTases. Site-directed mutagenesis of His-219 was carried out to replace the residue with asparagine and with glutamate. DNA sequencing confirmed the presence of the desired base changes and the absence of adventitious mutations. The mutant enzymes were overexpressed in the *nadA, pncB*-defective *S. typhimurium* strain RMS100. The enzymes were purified to near homogeneity as described for the wild-type enzyme (*27*), using SDS−PAGE to follow the purification. Typically, this protocol yielded 200 mg of protein from a 6 L culture.

Physical Properties of Mutant NAPRTases. The purified H219E and H219N enzymes were freed of buffers by reverse-phase HPLC and analyzed by electrospray mass spectrometry. The observed and predicted molecular masses of WT (45 542 ± 14 vs 45 529 Da), H219E (45 554 ± 8 vs 45 521 Da) and H219N (45 503 ± 20 vs 45 506 Da) were in good agreement and demonstrated that no proteolysis had occurred prior to purification. The H219E and H219N proteins were also subjected to gel-filtration chromatography on Superdex-75 and behaved similarly to the monomeric WT.

Functional Properties of Mutant NAPRTases. In wild-type NAPRTase, ATP hydrolysis is normally coupled to NAMN synthesis and can also be elicited by free PP_i. H219E and H219N showed no detectable (<0.005 unit/mg) NA-dependent or PP_i-stimulated ATP hydrolysis. Values for WT in the same experiments were 3.1 and 2.6 units/mg, respectively.

NAPRTase phosphorylated at His-219 is proposed to be an intermediate in the coupling of NAMN synthesis and ATP hydrolysis (*28*). The ability of H219E and H219N to autophosphorylate in the presence of ATP was tested. The phosphorylation stoichiometries for H219E and H219N were 0.01 and 0.003 mol of ^{32}P incorporated/mol of NAPRTase, respectively.

Another indicator of ATP utilization is the enzyme's ability to catalyze an ATP/ADP exchange in the absence of other substrates (*19*). The exchange rate for WT was 7.8 units/mg. H219E and H219N exchange rates were 0.13 and 0.3 unit/mg, respectively. These values, although low, were finite, and the exchanges were investigated further. It has been demonstrated that for the wild-type enzyme, PRPP inhibits the ADP/ATP exchange reaction (*19*). The presence of 1 mM PRPP decreased the exchange rate of WT to 0.2 unit/mg, whereas with H219E and H219N PRPP had no effect, suggesting that the slow exchange observed in the mutants might result from contamination of the mutant NAPRTases by a nucleotide kinase. Exchange reactions for WT, H219E, and H219N were also carried out in the presence of 10 μM P^1,P^5-di(adenosine-5′-) pentaphosphate (Ap5A), a potent inhibitor of adenylate kinase (*42*). The WT NAPRTase retained an exchange rate of 6 units/mg whereas H219E and H219N no longer showed any detectable exchange activity.

NAPRTase can also catalyze a slow but readily detected NAMN synthesis reaction in the absence of ATP (*19*). Under standard assay conditions (*19*), the rate of uncoupled NAMN synthesis for H219E was 1.5-fold slower and for H219N 3-fold slower than WT (not shown). Kinetic analysis showed that mutation of His-219 to glutamate or asparagine had not drastically affected the K_M for the substrate NA or the V_{max} in the uncoupled NAMN synthesis (Table 1). The K_M for PRPP was increased about 10-fold in H219N and was decreased 2-fold in H219E.

Table 1: Kinetic Parameters of H219E and H219N of *S. typhimurium* Nicotinate Phosphoribosyltransferase for Uncoupled NAMN Synthesis[a]

	K_M (mM)		
enzyme	NA	PRPP	V_{max} (units/mg)
WT	0.3 ± 0.1	4.5 ± 2.2	0.4 ± 0.09
H219E	0.33 ± 0.2	2.3 ± 0.9	0.3 ± 0.05
H219N	0.4 ± 0.2	48 ± 21	0.14 ± 0.04

[a] The kinetic data were fit to the hyperbolic form of the Michaelis−Menten equation with the aid of the program HYPER (*38*). The kinetic constants for the wild-type enzyme were determined under identical conditions by Vinitsky and Grubmeyer (*19*).

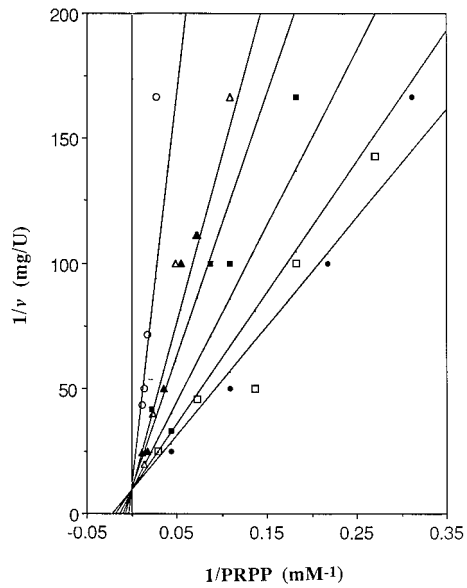

FIGURE 1: Competitive inhibition by ATP vs PRPP. Uncoupled NAMN synthesis activity was measured with ATP concentrations (●, 0 mM; □, 0.1 mM; ■, 0.3 mM; △, 0.7 mM; ▲, 1 mM; ○, 3 mM) and with increasing PRPP concentrations. The lines represent a computer fit to the data (*38*).

Inhibition of Uncoupled NAMN Synthesis by ATP. The mutant enzymes were tested for their ability to catalyze NAMN synthesis in the presence of 3 mM ATP. Under these conditions, NAMN formation by H219N was 0.001 unit/mg, 20-fold slower than the rate observed in the absence of ATP (0.02 unit/mg). The rate of H219E was slowed 1.5-fold. The inhibition of uncoupled NAMN synthesis by ATP in H219N was followed in detail by varying PRPP and ATP concentrations in the assay. The results (Figure 1) showed that ATP was a competitive inhibitor vs PRPP (K_I = 0.48 ± 0.11 mM).

ATP binding to H219N was detectable using equilibrium gel filtration. At enzyme concentrations of 250 μM and an [γ-^{32}P]ATP concentration of 200 μM, 0.22 mol of [γ-^{32}P]-ATP was bound/mol of NAPRTase. From this single point, we can calculate a K_D estimate of 0.5 mM, a value consistent with the K_I for ATP.

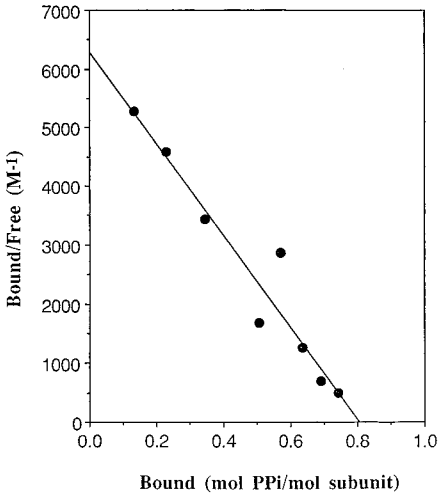

FIGURE 2: Scatchard plot of [^{32}P]PP_i binding to E. Binding was measured by equilibrium gel filtration. The line represents the least-squares fit.

PRPP and PP_i Binding to NAPRTase. The K_M of MgPRPP for WT NAPRTase in the uncoupled reaction (4.5 mM; *19*) suggests that the binding of MgPRPP is weak. In equilibrium gel-filtration experiments containing 100 μM [β-^{32}P]PRPP and 100 μM WT NAPRTase, 0.08 mol of [β-^{32}P]PRPP bound/mol of E was detected. The weak binding precluded further study. In the presence of ATP and Mg^{2+} (phosphorylation conditions), high-affinity PRPP binding to a single site is observed with WT enzyme (K_D = 0.5 μM; *36*). With His-219 mutant NAPRTase, no binding of [β-^{32}P]PRPP was detected, either in the presence or absence of ATP, under conditions in which a K_D as high as 2 mM would have been detected.

The K_D for [^{32}P]PP_i binding to unliganded WT NAPRTase, determined from a Scatchard plot analysis of equilibrium gel-filtration experiments, was 0.13 mM with 0.8 binding site/subunit (Figure 2). Equilibrium binding of [^{32}P]PP_i to WT NAPRTase in the presence of ATP and Mg^{2+} cannot be meaningfully measured due to the PP_i-stimulated ATPase activity of WT NAPRTase. The H219N mutant NAPRTase demonstrated weak [^{32}P]PP_i binding (K_D estimated to be 1.8 mM) in the absence of MgATP and no [^{32}P]PP_i binding in the presence of 3.0 mM ATP.

Proteolysis. WT NAPRTase is sensitive to trypsin, suffering a first-order activity loss in the presence of 1:200 trypsin/NAPRTase (w/w). Ligands MgATP and MgPRPP offer protection, individually and synergistically, against proteolysis (*27*). After 10 min of trypsin treatment, H219N lost 96% of the uncoupled NAMN synthesis activity. When the identical experiment was performed in the presence of 1 mM MgATP, 45% remaining activity was observed, representing a 4-fold increase in the $T_{1/2}$ for inactivation. The protection afforded by the presence of MgATP was not enhanced by the addition of 1 mM MgPRPP.

To define the trypsin cleavage site, H219N partially inactivated with trypsin in the presence and absence of ligands was purified by reverse-phase HPLC and analyzed by electrospray mass spectrometry. Comparison of the observed masses to theoretical values calculated from the known amino acid sequence (corrected for the mutation at His-219) (*10*) determined the cleavage sites. A major peptide with molecular mass of 43 868 Da was observed, suggesting cleavage at Arg-384 (theoretical value 43 826). Mutant enzyme treated with trypsin in the presence of MgATP, or MgATP with MgPRPP, gave two major peptides with observed molecular masses of 43 858 and 45 266 Da, suggesting cleavages at Arg-384 (43 826 Da) and Arg-396 (45 220 Da). These cleavage sites are identical to those for WT under the same conditions and show that binding of MgATP to the nonphosphorylatable H219N produces a similar confomational change as in WT.

PCR Subcloning and Overexpression of NPT1. The translated protein sequence of yeast NAPRTase is shown in Figure 3, together with the *Salmonella typhimurium* sequence (*10*) and the unpublished sequence of an open reading frame in *Mycobacterium tuberculosis* (GenBank accession number Z73902). The yeast sequence is 30% identical to that of the bacterial enzyme. The sequence from *M. tuberculosis*, a species thought to lack pyridine nucleotide recycling, shows weak overall similarity to the known NAPRTases but a higher degree of identity in several regions.

Restriction fragment and PCR-based methods were used to subclone yeast *npt1* from plasmid pFL44-RPB10f (*31*) into a T7 expression vector. High-level overexpression of active soluble protein was achieved when RMS12 was grown in LB containing 2% glycerol at 25 °C to OD_{600} = 0.6 and induced with 0.05% lactose (*43*). The protein was purified using the methods for the *S. typhimurium* enzyme. Reverse-phase HPLC of the purified protein, followed by amino-terminal protein sequencing over the first six residues, yielded the sequence H_2N-Ser-Glu-Pro-Val-Ile-Lys and confirmed the identity of the predicted protein in which the N-terminal methionine had been removed.

Functional Characterization of Yeast NAPRTase. Two groups (*44*−*46*) reported that the yeast enzyme catalyzed the NAMN synthesis reaction only in the presence of ATP, whereas *S. typhimurium* NAPRTase (*19*), like the mammalian enzyme (*18*), was shown to possess a slow uncoupled reaction as well. The recombinant yeast enzyme also catalyzed an uncoupled NAMN synthesis reaction, although, under the non-V_{max} assay conditions employed, it was 40-fold slower than the coupled rate (Table 2). Covalent phosphorylation of the recombinant yeast enzyme by [γ-^{32}P]-ATP [0.98 ($\pm$ 0.04) mol of ^{32}P/mol of enzyme] was also observed.

Earlier reports on NAPRTase from yeast (*46*) suggested that the reaction products NAMN and PP_i were each able to stimulate the ATPase reaction. In *S. typhimurium* NAPRTase only the PP_i-stimulated activity was observed (*19*). The ATPase activity of the recombinant yeast enzyme was also shown to be stimulated by either 1 mM NAMN or 1 mM PP_i (Table 3). Reexamination of the *S. typhimurium* NAPRTase showed that 1 mM NAMN could also stimulate a slow ATPase reaction by the enzyme.

DISCUSSION

The work presented here shows that mutagenesis of His-219, the proposed site of NAPRTase phosphorylation, inactivated ATP-linked functions of the enzyme. However, inactivation of the ATP usage did not destroy the weak ability of NAPRTase to synthesize NAMN in the absence of ATP. In these mutant enzyme forms, ATP acts as a competitive inhibitor, rather than a stimulator, of NAMN synthesis.

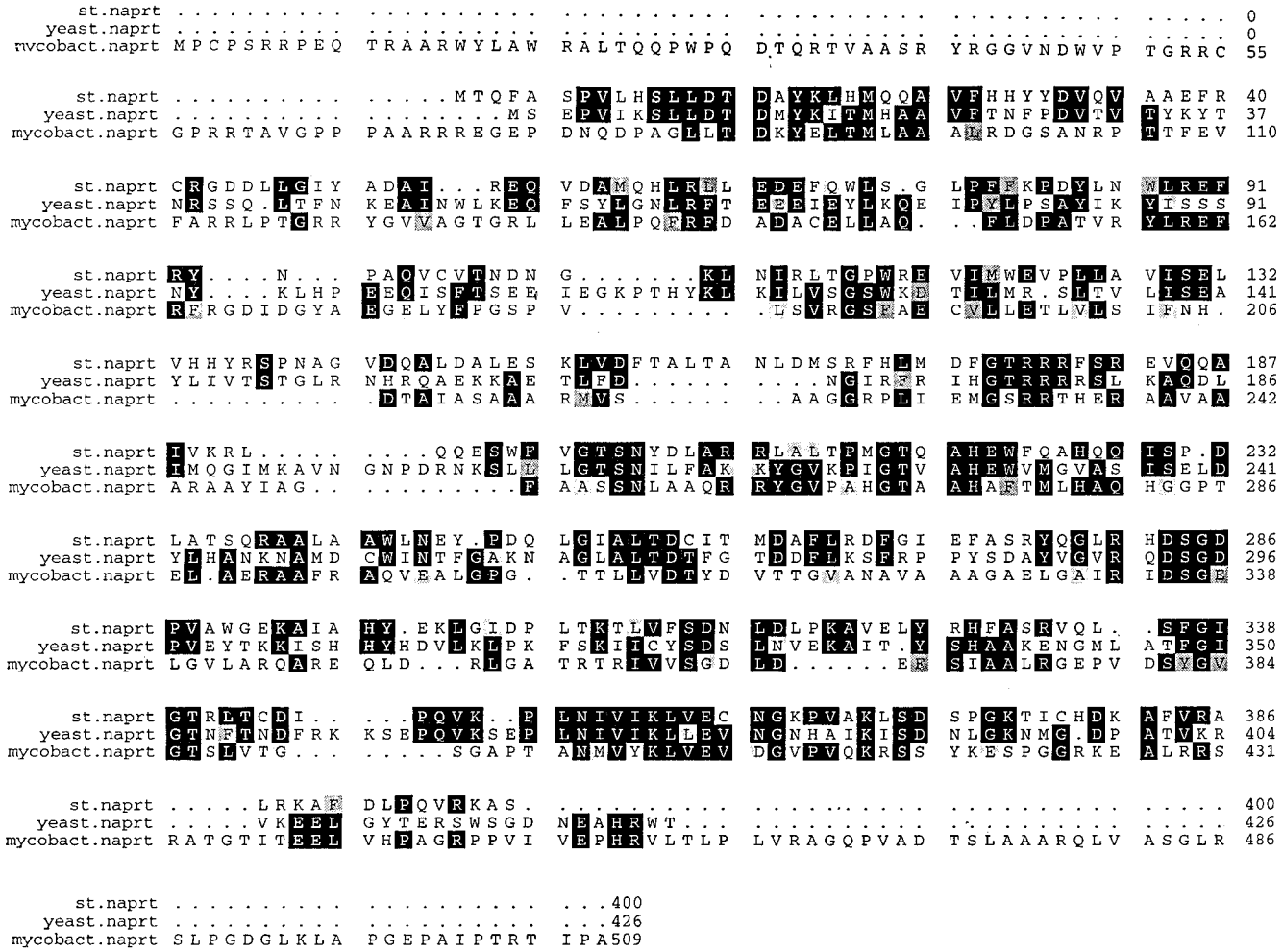

FIGURE 3: Alignment of coding sequences of NAPRTases. Alignments were done using the PILEUP program in the GCG package (University of Wisconsin, Madison, WI). The shaded areas show amino acid identities in all sequences. The species (and accession numbers) are *Salmonella typhimurium* (M55986), *Saccharomyces cerevisiae* (Z36878 and Z75117), and *Mycobacterium tuberculosis* (Z73902).

Table 2: Conversion of [^{14}C]NA to [^{14}C]NAMN by *Salmonella* and Yeast NAPRTases

	Coupled ATPase[a] (units/mg)	NAMN synthesis[b] (units/mg)	
		+ATP	−ATP
Salmonella	2.8	1.3	0.06
yeast	2.9	2.3	0.06

[a] Spectrophotometric assay as described by Vinitsky and Grubmeyer (*19*). [b] Separate radiotransfer assay as described by Vinitsky and Grubmeyer (*19*).

Table 3: ATP Hydrolysis Stimulated by Products PP_i and NAMN[a]

additions	yeast enzyme (units/mg)	*Salmonella* enzyme (units/mg)
+PRPP, +NA	2.9	3.1
+PP_i	0.65	1.8
+NAMN	0.43	0.3

[a] Coupled spectrophotometric assay was performed as described by Vinitsky and Grubmeyer (*19*).

When incubated with MgATP and MgPRPP, WT NAPRTase is phosphorylated at the N1 position of His-219 (*28*). The enzyme−phosphate bond was shown to be rapidly hydrolyzed in the presence of substrates for the NAMN synthesis reaction, as expected for a kinetically competent intermediate. Confirming the assigned role of His-219, both the H219N and H219E mutants were inactivated for substrate or PP_i-stimulated ATPase and for autophosphorylation. Although a weak ADP/ATP exchange was observed with preparations of the mutant NAPRTases, this was shown to result from an adenylate kinase contaminant and was not intrinsic to the mutant enzymes. Gel filtration and electrospray mass spectrometry showed that the low activity of the mutant enzymes was not the result of gross denaturation or proteolysis. In addition, ATP binding to the H219N mutant enzyme was detected with an estimated K_D of 0.5 mM.

In the normal reaction cycle, the presence of ATP triggers the tight binding of PRPP and NA. A protein conformational change in WT enzyme protects the carboxy terminus from proteolysis at Lys-384. This change occurs under phosphorylation conditions and when ATP is allowed to bind in the absence of Mg^{2+}, conditions under which the enzyme is not phosphorylated (*27*), suggesting that either phosphorylation or ATP binding alone promotes the protein conformational change that leads to protection. The MgATP protection against trypsin proteolysis observed with H219N, which is not phosphorylatable, further supports this conclusion.

In past work, it was not clear whether PRPP and ATP binding were mutually exclusive events. The analysis of the uncoupled NAMN synthesis reaction by H219N resolved this point. ATP was a good inhibitor of the NAMN synthesis

activity of H219N enzyme, competitive vs PRPP. The competitive inhibition could result from ATP occupancy of the PRPP binding site. This conclusion is strengthened by the previous observation of substrate inhibition by PRPP with the yeast enzyme (*29*). In addition, we have observed that the nonhydrolyzable ATP analogue AMP-PCP, which is a weak inhibitor of the ATP-linked functions of WT, also inhibits the uncoupled NAMN synthesis activity and the binding of [β-^{32}P]PRPP observed with WT (not shown). Here, we also found ATP inhibition of the weak PP_i binding by H219N. These results, taken together, strongly suggest that the binding site for ATP in part overlaps with those for PP_i and PRPP, probably through the pyrophosphate moiety shared by all three ligands.

Thus far, there are primary structures of only four NAPRTases: that from *S. typhimurium* (and its nearly identical *E. coli* homologue; *9*); the yeast enzyme reported here, and the *Mycobacterium tuberculosis* open reading frame identified from genome sequencing. The three show only limited overall similarity, but there is conservation of a number of residues, including His-219. The differences between the behavior of the yeast enzyme and that from *S. typhimurium*, as reported in the literature, suggested that fundamental differences in mechanism might exist between these enzyme forms, although the lengthy purification procedures and small amounts of the yeast enzyme might have generated artifacts. Here, we found that the yeast and bacterial enzymes display similar uncoupled NAMN synthesis and NAMN-stimulated ATPase reactions.

Currently, there is no three-dimensional structure for any NAPRTase. Two evolutionarily distinct structures, types 1 and 2, are known for PRTases (*12*). QAPRTase is the sole example of type 2, so that it is not yet possible to conclusively identify sequence motifs that characterize this enzyme group. Interestingly, QAPRTase also catalyzes the formation of NAMN, employing quinolinic acid as the base. Using the QAPRTase three-dimensional structure, the spacing and nature of residue identities between QAPRTase and NAPRTase conserved sequences provides tantalizing evidence that the two proteins are related. That similarity is shown here:

QAPRTases

TRKT- X_{19} -**HR**-X_{11}-**NH**-$X_{25/28}$-**E**-X_{20}-**D**

NAPRTases

TRRR-$X_{20/31}$-**SN**-X_{15}-**AH**-$X_{36/39}$-**D**-X_{24}-**D**

where the subscripted X designates the range of unconserved amino acids. The active site of QAPRTase is formed by a seven-stranded α/β barrel, and sequence conservation among known QAPRTases is strong at the tops of these β strands, where side chains interact with bound substrate. One sequence, 151-TRKT-154 (numbering is for the *S. typhimurium* enzyme), forms the top of strand B4, from which Arg-152 interacts with the 3-carboxylate of NAMN and Lys-153 interacts with the 5′-phosphate. This motif appears to be represented by a highly conserved area of *S. typhimurium* NAPRTase, 176-TRRR-179. Residues His-174 and Arg-175, absolutely conserved among QAPRTases, form the top of strand B5 and interact with the pyridine base. Two absolutely conserved residues occupy this position of NAPRTase, Ser-202 and Asn-203, and may interact with the differentially substituted base substrate of the enzyme. In QAPRTase, two carboxylate residues, Glu-214 and Asp-235, are conserved among all sequences. These residues are located at the top of strands B7 and B8 and their side chains interact with the 2′ and 3′ hydroxyl groups of bound NAMN, respectively. In NAPRTases, Asp-258 and Asp-283 are absolutely conserved and may be structural homologues. Finally, a residue of QAPRTase that is found at the carboxyl end of strand B6, His-188, is located directly across the active-site pocket from bound NAMN, in position to interact with PP_i. His-188 may be the structural homologue of His-219 of NAPRTase. QAPRTase is not detectably stimulated by ATP, and results suggesting the phosphorylation of QAPRTase (*11*) have not yet been confirmed.

ACKNOWLEDGMENT

We thank Dr. Pierre Thuriaux, CEA Saclay, for donating yeast clones. Mass spectroscopy was provided by Dr. William Moore at The Protein Chemistry Laboratory of the Medical School of the University of Pennsylvania supported by core grants of the Diabetes and Cancer Centers (DK-19520 and CA-16520). We are grateful to Mr. Yiming Xu for helpful discussions.

REFERENCES

1. Tritz, G. J. (1987) in *Escherichia coli and Salmonella typhimurium*: *Cellular and Molecular Biology* (Neidhardt, F. C., Ed.) pp 557−563, American Society for Microbiology Press, Washington, DC.
2. Penfound, T., and Foster, J. F. (1996) in *Escherichia coli and Salmonella typhimurium: Cellular and Molecular Biology* (Neidhardt, F. C., Ed.) 2nd ed., pp 721−730, American Society for Microbiology Press, Washington, DC.
3. Musick, W. D. L. (1981) *Crit. Rev. Biochem. 11*, 1−34.
4. Hove-Jenson, B., Harlow, K. W., King, C. J., and Switzer, R. L. (1986) *J. Biol. Chem. 261*, 6765−6771.
5. Hershey, V., and Taylor, M. W. (1986) *Gene 43*, 287−293.
6. Scapin, G., Grubmeyer, C., and Sacchettini, J. C. (1994) *Biochemistry 33*, 1287−1294.
7. Eads, J. C., Scapin, G., Xu, Y., Grubmeyer, C., and Sacchettini, J. C. (1994) *Cell 78*, 325−334.
8. Smith, J. L., Zaluzec, E. J., Wery, J., Niu, L., Switzer, R. L., Zalkin, H., and Satow, Y. (1994) *Science 264*, 1427−1433.
9. Wubbolts, M. G., Terpstra, P., van Beilen, J., Kingma, J., Meesters, H. A. R., and Witholt, B. (1990) *J. Biol. Chem. 265*, 17665−17672.
10. Vinitsky, A., Teng, H., and Grubmeyer, C. T. (1991) *J. Bacteriol. 173*, 536−540.
11. Hughes, K. T., Dessen, A., Gray, J. P., and Grubmeyer, C. (1993) *J. Bacteriol. 175*, 479−486.
12. Eads, J. C., Ozturk, D., Wexler, T. B., Grubmeyer, C., and Sacchettini, J. C. (1997) *Structure 5*, 47−58.
13. Imsande, J. (1964) *Biochim. Biophys. Acta 85*, 255−264.
14. Ogasawara, N., and Gholson, R. K. (1966) *Biochim. Biophys. Acta 118*, 422−431.
15. Honjo, T., Nakamura, S., Nishizuka, Y., and Hayaishi, O. (1966) *Biochem. Biophys. Res. Commun. 25*, 199−204.
16. Imsande, J., and Handler, P. (1961) *J. Biol. Chem. 236*, 525−530.
17. Smith, L. D., and Gholson, R. K. (1969) *J. Biol. Chem. 244*, 68−71.
18. Niedel, J., and Dietrich, L. S. (1973) *J. Biol. Chem. 248*, 3500−3505.
19. Vinitsky, A., and Grubmeyer, C. T. (1993) *J. Biol. Chem. 268*, 26004−26010.

20. Natalini, P., Ruggieri, S., Santarelli, I., Vita, A., and Magni, G. (1979) *J. Biol. Chem. 254*, 1558−1563.
21. Rasmussen, U. B., Mygind, B., and Nygaard, P. (1986) *Biochim. Biophys. Acta 881*, 268−275.
22. Tanford, C. (1983) *Annu. Rev. Biochem. 52*, 379−409.
23. Meek, T. D., and Villafranca, J. J. (1982) *Biochemistry 21*, 2158−2167.
24. Jencks, W. P. (1980) *Adv. Enzymol. 51*, 75−106.
25. Jencks, W. P. (1989) *J. Biol. Chem. 264*, 18855−18858.
26. Alberts, B., and Miake-Lye, R. (1992) *Cell 68*, 415−420.
27. Rajavel, M., Gross, J., Segura, E., Moore, W. T., and Grubmeyer, C. (1996) *Biochemistry 35*, 3909−3916.
28. Gross, J., Rajavel, M., Segura, E., and Grubmeyer, C. (1996) *Biochemistry 35*, 3917−3924.
29. Hanna, L., and Sloan, D. L. (1980) *Anal. Biochem. 103*, 230−234.
30. Xu, Y., Eads, J., Sacchettini, J. C., and Grubmeyer, C. (1997) *Biochemistry 36*, 3700−3712.
31. Lalo, D., Carles, C., Sentenac, A., and Thuriaux, P. (1993) *Proc. Natl. Acad. Sci. U.S.A. 90*, 5524−5528.
32. Tabor, S., and Richardson, C. (1985) *Proc. Natl. Acad. Sci. U.S.A. 82*, 1074−1078.
33. Sambrook, J., Fritsch, E. F., and Maniatis, T. (1989) *Molecular Cloning: A Laboratory Manual*, 2nd ed., Cold Spring Harbor Laboratory Press, Cold Spring Harbor, NY.
34. Ho, S. N., Hunt, H. D., Horton, R. M., Pullen, J. K., and Pease, L. R. (1989) *Gene 77*, 51−59.
35. Preiss, J., and Handler, P. (1958) *J. Biol. Chem. 233*, 492−500.
36. Gross, J. W., Rajavel, M., and Grubmeyer, C. (1998) *Biochemistry 37*, 4189−4199.
37. Penefsky, H. S. (1977) *J. Biol. Chem. 252*, 2891−2899.
38. Cleland, W. W. (1979) *Methods Enzymol. 63*, 103−139.
39. Hummel, J. P., and Dreyer, W. J. (1962) *Biochim. Biophys. Acta 63*, 530−532.
40. Scatchard, G. (1949) *Ann. N.Y. Acad. Sci. 51*, 660−672.
41. Vinitsky, A. (1991) Ph.D. Thesis, Department of Biology, New York University.
42. Lienhard, G. E., and Secemski, I. I. (1973) *J. Biol. Chem. 248*, 1121−1123.
43. Kopetzki, E., Schumacher, G., and Buckel, P. (1989) *Mol. Gen. Genet. 216*, 149−155.
44. Kosaka, A., Spivey, H. O., and Gholson, R. K. (1971) *J. Biol. Chem. 246*, 3277−3283.
45. Kosaka, A., Spivey, H. O., and Gholson, R. K. (1977) *Arch. Biochem. Biophys. 179*, 334−341.
46. Hanna, L. S., Hess, S. L., and Sloan, D. L. (1983) *J. Biol. Chem. 258*, 9745−9754.

BI9720134